Biochemistry and Biophysics Reports 5 (2016) 211–215

Contents lists available at ScienceDirect

Biochemistry and Biophysics Reports

journal homepage: www.elsevier.com/locate/bbrep

Visualization of biodistribution of Zn complex with antidiabetic activity using semiconductor Compton camera GREI

Masayuki Munekane [a,b], Shinji Motomura [c], Shinichiro Kamino [a,c], Masashi Ueda [a], Hiromitsu Haba [d], Yutaka Yoshikawa [e,1], Hiroyuki Yasui [e], Makoto Hiromura [c,2], Shuichi Enomoto [a,c,*]

[a] Graduate School of Medicine, Dentistry, and Pharmaceutical Sciences, Okayama University, 1-1-1 Tsushimanaka, Kita-ku, Okayama 700-8530, Japan
[b] Japan Society for the Promotion of Science, 5-3-1 Kojimachi, Chiyoda-ku, Tokyo 102-0083, Japan
[c] Next-generation Imaging Team, RIKEN Center for Life Science Technologies, 6-7-3 Minatojima-minamimachi, Chuo-ku, Kobe, Hyogo 650-0047, Japan
[d] RIKEN Nishina Center for Accelerator-Based Science, RIKEN, 2-1 Hirosawa, Wako, Saitama 351-0198, Japan
[e] Department of Analytical and Bioinorganic Chemistry, Division of Analytical and Physical Chemistry, Kyoto Pharmaceutical University, 5 Nakauchi-cho, Misasagi, Yamashina-ku, Kyoto 607-8414, Japan

ARTICLE INFO

Article history:
Received 28 September 2015
Received in revised form
24 November 2015
Accepted 7 December 2015
Available online 8 December 2015

Keywords:
GREI
^{65}Zn-labeled Zn complex
Biodistribution

ABSTRACT

Various types of zinc (Zn) complexes have been developed as promising antidiabetic agents in recent years. However, the pharmacological action of Zn complex is not elucidated because the biodistribution of the complex in a living organism has not been studied. Nuclear medicine imaging is superior technology for the noninvasive analysis of the temporal distribution of drug candidates in living organisms. Gamma-ray emission imaging (GREI), which was developed by our laboratory as a novel molecular imaging modality, was adopted to visualize various γ-ray–emitting radionuclides that are not detected by conventional imaging techniques such as positron emission tomography and single-photon emission computed tomography. Therefore, we applied GREI to a biodistribution assay of Zn complexes. In the present study, ^{65}Zn was produced in the ^{nat}Cu(p,n) reaction in an azimuthal varying field cyclotron for the GREI experiment. The distribution was then noninvasively visualized using GREI after the intravenous administration of a ^{65}Zn-labeled di(1-oxy-2-pyridinethiolato)zinc [Zn(opt)$_2$], $ZnCl_2$, and di(L-histidinato)zinc. The GREI images were validated using conventional invasive assays. This novel study showed that GREI is a powerful tool for the biodistribution analysis of antidiabetic Zn complexes in a living organism. In addition, accumulation of ^{65}Zn in the cardiac blood pool was observed for [Zn(opt)$_2$], which exhibits potent antidiabetic activity. These results suggest that the slow elimination of Zn from the blood is correlated to the antidiabetic activity of [Zn(opt)$_2$].

1. Introduction

Medicinal inorganic chemistry is a discipline in which metal complexes are used in therapeutic and diagnostic medicine [1–3]. The zinc (Zn) complexes are promising metallodrugs for the treatment of type 2 diabetes mellitus [4–5]. In recent years, several Zn complexes have been discovered that have potent antidiabetic activity in experimental diabetic animals [5–7]. For example, a novel Zn complex showed potent hypoglycemic activity at a dose lower than the clinical dose of zinc acetate used to treat Wilson's disease [7]. It is presumed that the Zn atom is the component of the complex responsible for its hypoglycemic activity since ligands such as low-molecular-weight organic compounds are generally inactive. The complexation of Zn with a ligand improves its gastrointestinal absorption, enabling its efficient delivery to target tissues [7–9]. The coordination mode of the Zn complex also influences its pattern of tissue distribution [9,10]. However, the pharmacological action of Zn complexes is not fully elucidated because their biodistribution *in vivo* has not been extensively studied. Therefore, the development of noninvasive methods for

Abbreviations: DM, Diabetes mellitus; GREI, Gamma-ray emission imaging; PET, Positron emission tomography; SPECT, Single-photon emission computed tomography; [Zn(opt)2], Di(1-oxy-2-pyridinethiolato)zinc; [Zn(His)2], Di(L-histidinato) zinc; DMSO, Dimethyl sulfoxide

* Corresponding author at: Graduate School of Medicine, Dentistry, and Pharmaceutical Sciences, Okayama University, 1-1-1 Tsushimanaka, Kita-ku, Okayama 700-8530, Japan.
E-mail address: semo@riken.jp (S. Enomoto).
[1] Present address: Department of Health, Sports, and Nutrition Faculty of Health and Welfare, Kobe Women's University, 4-7-2 Minatojima-nakamachi, Chuo-ku, Kobe 650-0046, Japan.
[2] Present address: Department of Hygienic Chemistry, Daiichi University of Pharmacy, 22-1 Tamagawa-cho, Minami-ku, Fukuoka 815-8511, Japan.

http://dx.doi.org/10.1016/j.bbrep.2015.12.004

analyzing the distribution of Zn complexes *in vivo* will accelerate the discovery of safe and efficacious Zn complexes for treatment of type 2 diabetes.

The nuclear medicine imaging technique is useful in early drug development for analyzing the biokinetics of drug candidates in experimental animals and humans (*i.e.*, clinical microdose studies) [11,12]. Positron emission tomography (PET) and single-photon emission computed tomography (SPECT) are widely used to non-invasively visualize the movements of radionuclide-labeled molecules [13,14]. However, PET is limited to determine 511 keV γ-rays that originate from positron-emitting radionuclide while PET is more sensitive and accurate than other molecular imaging techniques. In SPECT imaging, γ-rays with low energy (<300 keV) emitted from the radionuclide are detected. Therefore, these conventional apparatuses are not suitable for the measurement and visualization of the *in vivo* behavior of the Zn complex because ^{65}Zn chosen as a radionuclide for the labeling emits γ-ray with high energy of 1116 keV.

On the other hand, the gamma-ray emission imaging (GREI) apparatus developed in our laboratory enables the spectroscopic imaging of wide energy-range γ-rays (200–2000 keV) by using a semiconductor Compton camera system [15]. The *in vivo* imaging of different γ-ray–emitting radionuclides, such as $^{65}ZnCl_2$, $^{85}SrCl_2$, iodinated (^{131}I) methylnorcholesterol and others, was achieved using GREI [15–17]. Successful demonstrations of the multiple molecular imaging inspired us to apply GREI to the biodistribution analysis of the Zn complex in a living organism. This study was the first to noninvasively investigate the kinetic behaviors of the di(1-oxy-2-pyridinethiolato)zinc complex ([Zn(opt)$_2$]), which has potent antidiabetic activity, using GREI after an intravenous administration of ^{65}Zn-labeled [Zn(opt)$_2$]. The distribution was compared to those of $ZnCl_2$ and the di(L-histidinato)zinc complex ([Zn(His)$_2$]), which does not exhibit antidiabetic activity.

2. Experimental

2.1. Animals

Ten-week-old male C57BL/6J mice were purchased from CLEA Japan, Inc. All animals were housed under a 12-h light/dark cycle in a temperature-controlled animal room and were allowed free access to food and tap water. All animal experiments were approved by the Ethics Committee on Animal Care and Use of RIKEN and were performed in accordance with the Guide for the Care and Use of Laboratory Animals.

2.2. Probe preparation

The ^{65}Zn nuclide was produced in the ^{nat}Cu(p,n) reaction (nat: natural isotopic abundance) in a RIKEN azimuthal varying field cyclotron. A metallic copper foil (chemical purity: 99.99%) 220 mg/cm^2 thick was irradiated by a 14-MeV proton beam with an intensity of 15 μA. After the irradiation, ^{65}Zn was chemically separated from the Cu target by an anion-exchange method. Radionuclide purity $>99\%$ was determined by the γ-ray spectrometry using a calibrated Ge detector. The specific radioactivity >0.2 GBq/g was estimated by inductively coupled plasma mass spectrometry for a control sample that was treated with the same chemical process as the irradiated Cu target.

[Zn(opt)$_2$] and [Zn(His)$_2$] were prepared as previously described [8,18], and the complexes were determined by elemental analyses and infrared spectra. Their predicted coordination structures are shown in Fig. 1 [19,20].

Purified ^{65}Zn dissolved in 30 μL of saline (Otsuka Pharmaceutical Co. Ltd.) and [Zn(opt)$_2$] dissolved in 70 μL of dimethyl sulfoxide (DMSO; Wako Pure Chemical Industries Ltd.) or [Zn(His)$_2$] dissolved in 70 μL of saline were stirred at room temperature over night to exchange cold Zn and ^{65}Zn [7,9,10]. The $^{65}ZnCl_2$ solution, a mixture of ^{65}Zn dissolved in 30 μL of saline and $ZnCl_2$ dissolved in 70 μL of DMSO, was prepared immediately prior to administration. The solutions were prepared to contain 10 mg Zn/mL as well as 10 MBq/mL or 2.5 MBq/mL for the GREI experiment or biodistribution analysis, respectively.

2.3. GREI experiment

Eleven-week-old male C57BL/6J mice were intravenously administered a single dose of ^{65}Zn-labeled [Zn(opt)$_2$] ([^{65}Zn(opt)$_2$]), ^{65}Zn-labeled $ZnCl_2$ ($^{65}ZnCl_2$), or ^{65}Zn-labeled [Zn(His)$_2$] ([^{65}Zn(His)$_2$]) *via* the tail vein at 1.0 mg Zn/kg of body weight. Each mouse was fixed on a board and placed just under the imaging head. Fifteen minutes after the injection, the GREI experiments were carried out under isoflurane anesthesia for 8 h. The acquired data were recorded in list mode with real-, and live-time information. The distribution images were reconstructed from the acquired data by the adoption of the image-reconstruction methods as previously described [15].

2.4. Biodistribution analysis

Eleven-week-old male C57BL/6J mice were divided into [^{65}Zn(opt)$_2$]-, $^{65}ZnCl_2$-, and [^{65}Zn(His)$_2$]-treated groups, and the ^{65}Zn-labeled compounds were intravenously administered at a dose of 1.0 mg Zn/kg of body weight. Four hours after the single intravenous administration, the mice were sacrificed under isoflurane anesthesia. Blood was collected, and the organs of interest (heart, pancreas, liver, kidney, stomach) were removed. Their radioactivities due to ^{65}Zn were measured using a calibrated Ge detector.

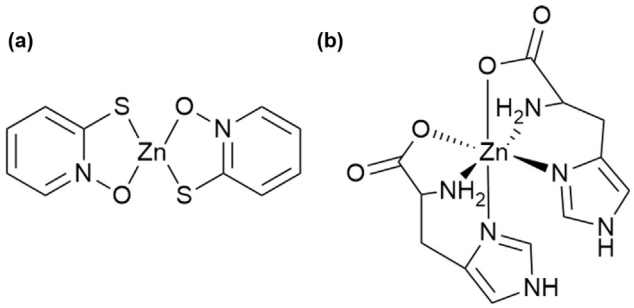

Fig. 1. Proposed coordination structures of the di(1-oxy-2-pyridinethiolato)Zn and di(L-histidinato)Zn complexes. Charges are omitted for simplicity.

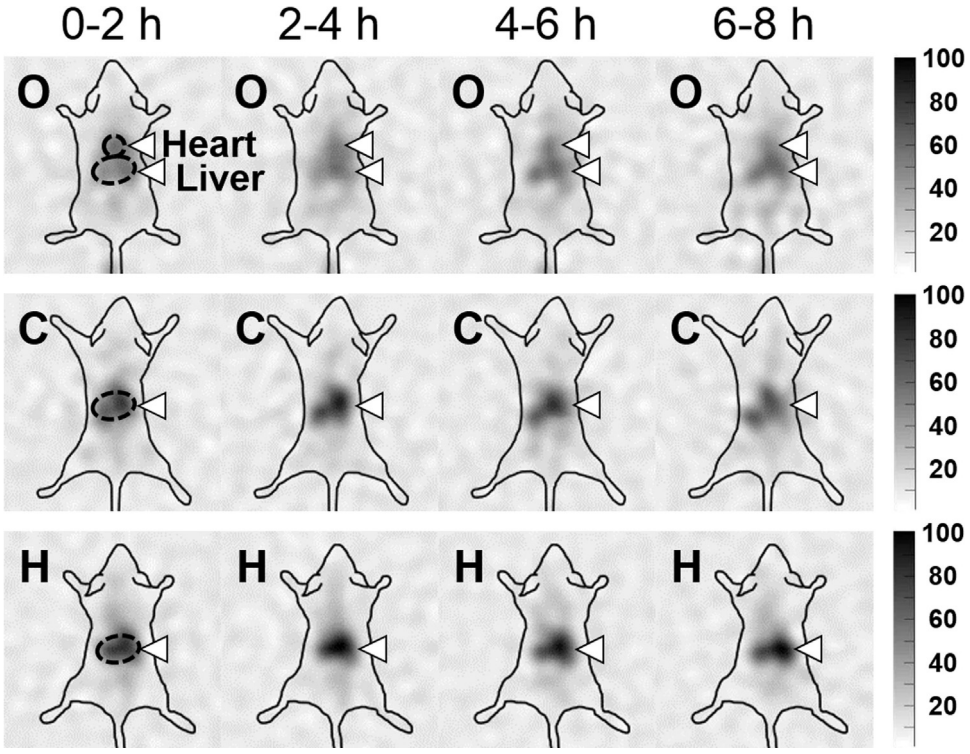

Fig. 2. Distribution images of ^{65}Zn in C57BL/6J mice after the administration of the ^{65}Zn-labeled Zn compounds ([^{65}Zn(opt)$_2$] (O), ^{65}ZnCl$_2$ (C), or [^{65}Zn(His)$_2$] (H)) reconstructed every 2 h. The arrows indicate the characteristic accumulation of ^{65}Zn.

3. Results

3.1. Visualization of ^{65}Zn-labeled Zn complexes in the whole body by GREI

The distribution images of ^{65}Zn were reconstructed every 2 h after the administration of [^{65}Zn(opt)$_2$], ^{65}ZnCl$_2$, or [^{65}Zn(His)$_2$] (Fig. 2). The arrows indicate the characteristic accumulation of ^{65}Zn. High accumulation of all compounds was observed in the liver. Moreover, a different distribution of ^{65}Zn among the studied Zn compounds was obtained in the distribution images: in the heart, high accumulation of [^{65}Zn(opt)$_2$] was noted, whereas little accumulation was observed for ^{65}ZnCl$_2$ and [^{65}Zn(His)$_2$].

The regions of interest were drawn around the heart and liver and the numerical values of the distributions was calculated by integrating the pixel values inside them to compare the values in the heart and liver of each mouse (Fig. 3). Image intensity gradients in such organs for each compound were maintained for 8 h and indicated that ^{65}Zn accumulation for [^{65}Zn(opt)$_2$] was much higher in the heart and lower in the liver than those for other studied compounds.

3.2. Biodistribution of ^{65}Zn

The radioactivities due to ^{65}Zn in the resected organs and blood were determined 4 h after the administration of [^{65}Zn(opt)$_2$], ^{65}ZnCl$_2$, or [^{65}Zn(His)$_2$] (Fig. 4). As shown in Fig. 4a, the uptake of ^{65}Zn in the liver was the highest, whereas the uptake rate (expressed as percent injected dose [%ID]) in the liver was at least twice as high as those in other organs for all compounds. The uptake rate of ^{65}Zn in the liver, pancreas, and kidney of [^{65}Zn(opt)$_2$]-treated mice were reduced compared with the uptake

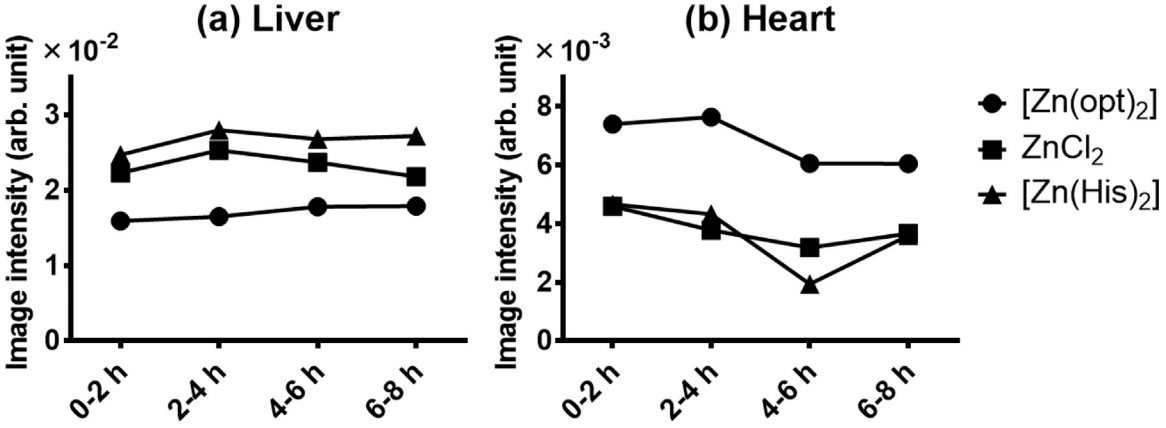

Fig. 3. Image intensities of the ^{65}Zn accumulated in the liver (a) and heart (b) extracted from each time flame of the images for [^{65}Zn(opt)$_2$], ^{65}ZnCl$_2$, and [^{65}Zn(His)$_2$].

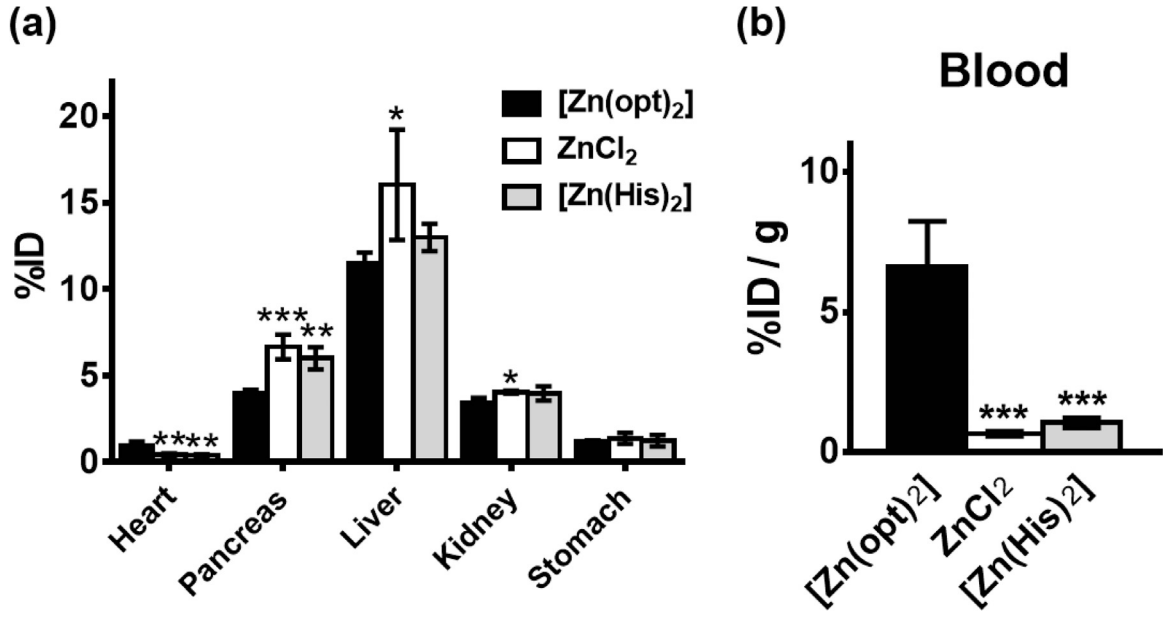

Fig. 4. The uptake rate of ^{65}Zn in each tissue (a) and in the blood (b) at 4 h after an intravenous administration of di(1-oxy-2-pyridinethiolato)Zn ([^{65}Zn(opt)$_2$]), ^{65}ZnCl$_2$, or di(L-histidinato)Zn ([^{65}Zn(His)$_2$]). Data are expressed as mean values ± SD for four mice. For the statistical evaluation, one-way analysis of variance with Bonferroni's test was used. $^{*}P < 0.05$, $^{**}P < 0.01$, $^{***}P < 0.001$ *versus* [^{65}Zn(opt)$_2$]. %ID, percent injected dose.

rate in each organ of ^{65}ZnCl$_2$- and [^{65}Zn(His)$_2$]-treated mice. On the other hand, the uptake rate in the heart tissue of [^{65}Zn(opt)$_2$]-treated mice was significantly higher than those of ^{65}ZnCl$_2$- and [^{65}Zn(His)$_2$]-treated mice. In addition, the concentration of ^{65}Zn (expressed as %ID/g tissue) in blood samples as [^{65}Zn(opt)$_2$] was much higher than that as ^{65}ZnCl$_2$ or [^{65}Zn(His)$_2$] (Fig. 4b).

4. Discussion

Biodistribution analyses of drug candidates enable the evaluation and prediction of their biological effects. For the assessment of the Zn complexes, tissue distribution patterns of exogenous Zn have been invasively analyzed by the determination of ^{65}Zn radioactivity in each tissue removed from the experimental animals after the administration of the ^{65}Zn-labaled Zn complex [7,9,10]. In general, the conventional method requires much time, high cost, and significant labor to assess drug candidate distribution. On the other hand, the molecular imaging technique enables a noninvasive and temporary study in the same living animals, decreases its statistical variance, and reduces the number of subjects. Therefore, we developed a noninvasive method for analyzing the distribution of ^{65}Zn-labeled Zn complexes in live mice using GREI. The conventional invasive assays were also performed to validate the GREI images.

In GREI experiments, we were the first to successfully visualize the difference in distribution among the ^{65}Zn-labeled compounds after their intravenous injection (Fig. 2). The distribution images of ^{65}Zn for all compounds in the liver and heart were in agreement with the results of the invasive assay (Figs. 3 and 4). The accumulation of ^{65}Zn increased in the liver of ^{65}ZnCl$_2$- and [^{65}Zn(His)$_2$]-treated mice, while the image intensities in the [^{65}Zn(opt)$_2$]-treated mouse was low. This tendency was also observed in the uptake rate of ^{65}Zn in the liver by the invasive assay. In addition, the accumulation of ^{65}Zn in the heart of [^{65}Zn(opt)$_2$]-treated mouse observed in the GREI image corresponds to the results that both ^{65}Zn blood concentration and ^{65}Zn uptake into the heart tissue in [^{65}Zn(opt)$_2$]-treated mice were higher than those in ^{65}ZnCl$_2$-, [^{65}Zn(His)$_2$]-treated mice. It is well known that the values of the thoracic pool (blood volume in the heart and lungs) amount to about 30% of the total circulatory blood volume [21]. The accumulation in the heart would be mainly derived from the enormously high concentration of ^{65}Zn in the blood of [^{65}Zn(opt)$_2$]-treated mice because the uptake rates of ^{65}Zn in the heart tissue were low. These results suggest that the distribution images of ^{65}Zn reflected the biodistributions determined by the invasive method.

Interestingly, the characteristic accumulation of ^{65}Zn was observed in the heart of [^{65}Zn(opt)$_2$]-treated mouse. The invasive assay exhibited that the accumulation was mainly derived from the radioactivity of ^{65}Zn in the cardiac blood pool. It was reported that a relatively long retention time of ^{65}Zn in the blood leads to a sustained release of Zn, which may be an important factor in the exertion of its antidiabetic activity [7,10]. The presented results suggested that the slow elimination of Zn from blood is related to the high antidiabetic activity of [Zn(opt)$_2$].

In conclusion, here we successfully demonstrated that GREI enables the noninvasive analysis of ^{65}Zn distribution for [^{65}Zn(opt)$_2$], ^{65}ZnCl$_2$, and [^{65}Zn(His)$_2$] in intact live mice as well as the visualization of the differences in ^{65}Zn distribution among these compounds. The accumulation of ^{65}Zn in the cardiac blood pool was observed for [Zn(opt)$_2$] as an antidiabetic drug candidate and suggested that the slow elimination of Zn from the blood may be an important factor related to its antidiabetic activity. We are currently investigating the correlation between the distribution pattern of the Zn complex and its antidiabetic activity, in addition to developing the GREI system to realize faster and more quantitative imaging analyses.

Acknowledgment

This work was supported by a Grant-in-Aid for the Japan Society for the Promotion of Science Fellows to M. Munekane (No. 26 · 8219).

Appendix A. Supplementary material

Supplementary data associated with this article can be found in the online version at http://dx.doi.org/10.1016/j.bbrep.2015.12.004.

References

[1] N. Farrell, Metal complexes as drugs and chemotherapeutic agents, Chem. Soc. Rev. Compr. Coord. Chem. II 9 (2003) 809–840.
[2] H. Sakurai, Y. Yoshikawa, H. Yasui, Current state for the development of metallopharmaceutics and anti-diabetic metal complexes, Chem. Soc. Rev. 37 (2008) 2383–2392.
[3] A. Bergamo, C. Gaiddon, J.H.M. Schellens, J.H. Beijnen, G. Sava, Approaching tumour therapy beyond platinum drugs: Status of the art and perspectives of ruthenium drug candidates, J. Inorg. Biochem. 106 (2012) 90–99.
[4] H. Sakurai, A. Katoh, T. Kiss, T. Jakusch, M. Hattori, Metallo-allixinate complexes with anti-diabetic and anti-metabolic syndrome activities, Metallomics 2 (2010) 670–682.
[5] Y. Yoshikawa, H. Yasui, Zinc complexes developed as metallopharmaceutics for treating diabetes mellitus based on the bio-medicinal inorganic chemistry, Curr. Top. Med. Chem. 12 (2012) 210–218.
[6] S. Kadowaki, M. Munekane, Y. Kitamura, M. Hiromura, S. Kamino, Y. Yoshikawa, H. Saji, S. Enomoto, Development of new zinc dithiosemicarbazone complex for use as oral antidiabetic agent, Biol. Trace Elem. Res. 154 (2013) 111–119.
[7] S. Fujimoto, H. Yasui, Y. Yoshikawa, Development of a novel antidiabetic zinc complex with an organoselenium ligand at the lowest dosage in KK-A^y mice, J. Inorg. Biochem. 121 (2013) 10–15.
[8] Y. Yoshikawa, A. Murayama, Y. Adachi, H. Sakurai, H. Yasui, Challenge of studies on the development of new Zn complexes ($Zn(opt)_2$) to treat diabetes mellitus, Metallomics 3 (2011) 686–692.
[9] Y. Adachi, J. Yoshida, Y. Kodera, T. Kiss, T. Jakusch, E.A. Enyedy, Y. Yoshikawa, H. Sakurai, Oral administration of a zinc complex improves type 2 diabetes and metabolic syndromes, Biochem. Biophys. Res. Commun. 351 (2006) 165–170.
[10] H. Murakami, H. Yasui, Y. Yoshikawa, Pharmacological and pharmacokinetic studies of anti-diabetic tropolonato-Zn(II) complexes with $Zn(S_2O_2)$ coordination mode, Chem. Pharm. Bull. 60 (9) (2012) 1096–1104.
[11] P.M. Matthews, E.A. Rabiner, J. Passchier, R.N. Gunn, Positron emission tomography molecular imaging for drug development, Br. J. Clin. Pharmacol. 73 (2011) 175–186.
[12] C.C. Wagner, O. Langer, Approaches using molecular imaging technology – use of PET in clinical microdose studies, Adv. Drug Deliv. Rev. 63 (2011) 539–546.
[13] J.K. Willimann, N. van Bruggen, L.M. Dinkelborg, S.S. Gambhir, Molecular imaging in drug development, Nat. Rev. Drug Discov. 7 (2008) 591–607.
[14] P. Ray, Multimodality molecular imaging of disease progression in living subjects, J. Biosci. 36 (2011) 499–504.
[15] S. Motomura, S. Enomoto, H. Haba, K. Igarashi, Y. Gono, Y. Yano, Gamma-ray Compton imaging of multitracer in biological samples using strip germanium telescope, IEEE Trans. Nucl. Sci. 54 (2007) 710–717.
[16] S. Motomura, Y. Kanayama, H. Haba, Y. Watanabe, S. Enomoto, Multiple molecular simultaneous imaging in a live mouse using semiconductor Compton camera, J. Anal. At. Spectrom. 23 (2008) 1089–1092.
[17] S. Motomura, Y. Kanayama, M. Hiromura, T. Fukuchi, T. Ida, H. Haba, Y. Watanabe, S. Enomoto, Improved imaging performance of a semiconductor Compton camera GREI makes for a new methodology to integrate bio-metal analysis and molecular imaging technology in living organisms, J. Anal. At. Spectrom. 28 (2013) 934–939.
[18] Y. Yoshikawa, E. Ueda, Y. Suzuki, N. Yanagihara, H. Sakurai, Y. Kojima, New insulinomimetic zinc(II) complexes of α-amino acids and their derivatives with $Zn(N_2O_2)$ coordination mode, Chem. Pharm. Bull. 49 (2001) 652–654.
[19] B.L. Barnett, H.C. Kretschmar, F.A. Hartman, Structural characterization of bis (N-oxopyridine-2-thionato)zinc(II), Inorg. Chem. 16 (1977) 1834–1838.
[20] R.H. Kretsinger, F.A. Cotton, The crystal and molecular structure of di-(L-histidino)-zinc(II) dihydrate, Acta Cryst. 16 (1963) 651–657.
[21] G. Nylin, H. Celander, Determination of blood volume in the heart and lungs and the cardiac output through the injection of radiophosphorus, Circulation 1 (1950) 76–83.